Analytical Biochemistry 419 (2011) 53–60

Contents lists available at SciVerse ScienceDirect

Analytical Biochemistry

journal homepage: www.elsevier.com/locate/yabio

Real-time monitoring of matrix metalloproteinase-9 collagenolytic activity with a surface plasmon resonance biosensor

Atsushi Shoji, Mitsutaka Kabeya, Masao Sugawara *

Department of Chemistry, College of Humanities and Sciences, Nihon University, Sakurajousui, Setagaya, Tokyo 156-8550, Japan

ARTICLE INFO

Article history:
Received 8 June 2011
Received in revised form 23 July 2011
Accepted 25 July 2011
Available online 30 July 2011

Keywords:
Matrix metalloproteinase-9
Collagen IV
Surface plasmon resonance
Collagenolytic activity
Kinetic parameters

ABSTRACT

We describe a simple method for real-time monitoring of matrix metalloproteinase-9 (MMP-9) collagenolytic activity for native triple helical collagen IV with a surface plasmon resonance (SPR) biosensor. The proteolytic activity of MMP-9 is measured as a decrease in the SPR signal resulting from the cleavage of collagen IV immobilized on the sensor surface. The kinetic parameters of full-length MMP-9 and its catalytic domain—catalytic constant (k_{cat}), association rate constant (k_a), and dissociation rate constant (k_d)—were estimated by the SPR method. The presence of sodium chloride and a nonionic detergent Brij-35 in a reaction solution led to the lower collagenolytic activity of MMP-9, whereas they suppressed the nonspecific interaction between MMP-9 and a cysteamine-modified chip. The comparison of kinetic parameters between MMP-9 and its catalytic domain revealed that the association constant of MMP-9 is much larger than that of the catalytic domain, suggesting that the interplay among hemopexin-like domain, fibronectin type II repeats motif, and linker region (O-glycosylated domain) plays an important role in recognizing collagen IV.

Collagens are fundamental components of the extracellular matrix (ECM)[1] that provide mechanical strength and structural integrity to various tissues. Collagen molecules are composed of three α-chains of primarily repeating Gly-Xaa-Yaa triplets, which induces each α-chain to adopt a left-handed poly-pro-II helix. Three α-chains then intertwine to form a right-handed triple helical coiled coil [1,2]. This triple helical conformation renders collagen relatively resistant to degradation by many mammalian proteases, but matrix metalloproteinases (MMPs) can catalyze the hydrolysis of the triple helical collagen. In the basement membranes (BM), a specialized form of the ECM, collagen IV is a major constituent and can be degraded by MMP-9. The measurement of MMP-9 proteolytic activity degrading triple helical collagen IV (i.e., collagenolytic activity) is important for understanding the mechanism of BM remodeling and aberrant collagen catabolism in pathological conditions such as atherosclerosis, cancer, and rheumatoid arthritis [3–8]. In addition, MMP-9 has attracted much attention for its unique structure in which there are two collagen binding sites (i.e., three fibronectin type II repeats motif and C-terminal hemopexin-like domain), in contrast to other MMP family members containing only C-terminal hemopexin-like domain as a binding site [9–11].

The proteolytic activity of MMPs has been measured by the zymographic method [12–16], which is based on the electrophoresis of MMPs through polyacrylamide gels containing a copolymerized substrate such as collagen [17], gelatin (denatured collagen) [18–21], and casein [22]. After the electrophoretic separation under denaturing conditions with sodium dodecyl sulfate (SDS), the MMPs are renatured by exchange of SDS for a nonionic detergent such as Triton X-100. However, it is known that the refolding of MMPs recovers only part of the original activity. In addition, evaluating kinetics of proteolytic MMP activity is difficult.

A continuous assay method that uses an increase in fluorescence on hydrolysis, allowing evaluation of kinetics of MMP proteolytic activity, has been reported [23–33]. The method uses collagen-like synthetic peptides that include collagen sequences surrounding MMP cleavage sites. According to typical protocols of the assay, a nonionic detergent Brij-35 is added at nearly 5-fold concentration higher than the critical micelle concentration in order to minimize the nonspecific interaction between MMPs and the hydrophobic plastic surface. However, it was reported that Brij-35 affects the proteolytic behavior of MMPs [16,34].

* Corresponding author. Fax: +81 3 5317 9433.
E-mail address: sugawara@chs.nihon-u.ac.jp (M. Sugawara).

[1] *Abbreviations used:* ECM, extracellular matrix; MMP, matrix metalloproteinase; BM, basement membrane; SDS, sodium dodecyl sulfate; SPR, surface plasmon resonance; PAGE, polyacrylamide gel electrophoresis; MMP-9 CAT, MMP-9 catalytic domain; SPDP, *N*-succinimidyl 3-(2-pyridyldithio) propionate; TCEP, tris(2-carboxyethyl)phosphine; Tris, tris(2-carboxyethyl)phosphine hydrochloride; EDC, 1-ethyl-3-[3-(dimethylamino)propyl]carbodiimide hydrochloride; Hepes, 2-[4-(2-hydroxyethyl)-1-piperazinyl]ethanesulfonic acid; EDTA, ethylenediamine-*N,N,N′,N″*-tetraacetic acid disodium salt; NHS, *N*-hydroxysuccinimide; Tween 20, polyoxyethylene sorbitan monolaurate; DMSO, diemethyl sulfoxide; CD, circular dichroism; RU, response units; THP, triple helical peptide; S/N, signal/noise; CMC, critical micelle concentration.

0003-2697/$ - see front matter © 2011 Elsevier Inc. All rights reserved.
doi:10.1016/j.ab.2011.07.031

Furthermore, the enzymatic digestion of synthetic peptides only partially mimics the collagenolysis because the sequence of synthetic peptide is different from the native triple helical collagen sequence [14,16].

Recently, several researchers have demonstrated the potential application of surface plasmon resonance (SPR) biosensors to the measurement of a reaction between protease in a bulk solution and an immobilized substrate on the sensor surface. Aldinger and coworkers used an SPR biosensor for assay of endoproteolytic enzyme IgAse [35]. This method is based on the measurement of a decrease in the SPR signal resulting from the cleavage of the immobilized substrate by protease reaction. Wangkam and coworkers investigated the topology of protein surface that was digested by protease using atomic force microscopy (AFM) and showed that the SPR signal decrease is proportional to the amount of the digested substrate [36]. Measurements of MMP-3 activity [37] and caspase activity [38,39] have also been reported. These reports demonstrate that an SPR bsiosensor has a strong potential for the measurement of protease activity. On the other hand, few researchers have attempted to estimate the kinetic parameters using an SPR biosensor [40–43]. Corn and coworkers proposed a novel approach toward the quantitative analysis of enzyme-catalyzed surface reactions that follow both Langmuir adsorption kinetics and the Michaelis–Menten concept [41–43]. They found that kinetic parameters of an enzymatic reaction can be evaluated by monitoring an SPR signal.

In the current article, we describe an SPR method for evaluating MMP-9 activity for degrading triple helical collagen IV. Evaluation of kinetics of degrading native collagen IV is important for understanding collagenolysis; however, few studies have been reported on measurements of MMP-9 activity using triple helical collagen IV as a substrate. Gioia and coworkers estimated kinetic parameters, such as catalytic constant (k_{cat}) and Michaelis constant (K_m), of α-chain within collagen IV using a laser densitometer after SDS–PAGE (polyacrylamide gel electrophoresis) separation of collagen IV processed by MMP-9 [44], although kinetic parameters of degrading triple helical collagen IV by MMP-9 have not been investigated in detail. We attempted to determine the kinetic parameters for degrading triple helical collagen IV by full-length MMP-9 and its catalytic domain (MMP-9 CAT). The parameters obtained were compared with each other in terms of recognizing triple helical collagen IV.

Materials and methods

Reagents

Full-length human MMP-9 active form (2 μg/ml) was obtained from Life Laboratory (Yamagata, Japan). Human collagen type IV was purchased from Cosmo Bio (Tokyo, Japan). Catalytic domain of human MMP-9 (40 μg/ml solution) was obtained from Funakoshi (Tokyo, Japan). *N*-Succinimidyl 3-(2-pyridyldithio) propionate (SPDP) was obtained from Thermo Fisher Scientific (St. Worcester, MA, USA). Cysteamine, Brij-35, tris(2-carboxyethyl)phosphine (TCEP), and tris(2-carboxyethyl)phosphine hydrochloride (Tris) were purchased from Sigma Chemical (St. Louis, MO, USA). 1-Ethyl-3-[3-(dimethylamino)propyl]carbodiimide hydrochloride (EDC), 2-[4-(2-hydroxyethyl)-1-piperazinyl]ethanesulfonic acid (Hepes), and ethylenediamine-*N,N,N′,N′*-tetraacetic acid disodium salt (EDTA) were obtained from Dojindo Laboratories (Kumamoto, Japan). *N*-Hydroxysuccinimide (NHS), polyoxyethylene sorbitan monolaurate (Tween 20), sodium acetate trihydrate, sodium chloride, and boric acid were obtained from Wako Chemicals (Osaka, Japan). Milli-Q water (Millipore reagent water system, Bedford, MA, USA) was used throughout the experiments.

Apparatus

A BIAcore 2000 (Biacore, GE Healthcare, Berkshire, UK) was used for SPR measurements with a CM5 sensor chip (carboxymethylated dextran attached on the gold-coated glass surface). The operating temperature was 37 ± 0.1 °C. The pH of buffer solutions was adjusted with a glass electrode pH meter (model IOL-30, Denki Kagaku Keiki, Tokyo, Japan).

Preparation of SPDP-modified collagen IV

Collagen IV was dissolved in a 10-mM sodium acetate buffer solution (pH 4.0) to give a 2.0-mg/ml solution and was diluted by two times with a 0.10-M sodium phosphate buffer (pH 7.4) containing 0.10 M NaCl. A 0.30-ml portion of the solution was mixed with 3.7 μl of 20 mM SPDP in dimethyl sulfoxide (DMSO, anhydrous). Then the mixture was incubated for 1 h at room temperature, and unreacted SPDP was removed and replaced by a 10-mM sodium acetate buffer solution (pH 3.0) using ultrafiltration (Microcon YM-50, Millipore). The activated collagen IV is hereafter abbreviated as SPDP–collagen IV.

CD spectroscopy

Circular dichroism (CD) studies were carried out on a JA750 spectrometer (Jasco, Tokyo, Japan) equipped with a temperature control unit (Jasco PTC-348). Temperature-induced stability of 1 mg/ml native collagen IV and SPDP–collagen IV, each dissolved in a 50-mM Tris buffer solution (pH 7.4), was monitored by far-ultraviolet (UV) CD spectroscopy using a 1.0-cm path length quartz cell. Thermal transition caves were obtained by recording the molar ellipticity (θ) at 221 nm while the temperature was increased continuously from 20 to 75 °C at a rate of 0.2 °C/min.

Immobilization of SPDP–collagen IV on a CM5 sensor chip

SPDP–collagen IV was immobilized on a sensor chip in a flow system through formation of a disulfide crosslink. First, a CM5 sensor chip was equilibrated with a running solution consisting of 0.15 M NaCl, 10 mM Hepes/NaOH (pH 7.4), 3.4 mM EDTA, and 0.005% Tween 20 (filtered through 0.2-μm membrane filter, abbreviated as a HBS–EP solution). Next, the CM5 sensor chip was activated by injecting a mixture of 0.1 M NHS and 0.4 M EDC in water for 7 min at a flow rate of 5 μl/min. A 0.1-M borate buffer solution (pH 8.5) containing 40 mM cysteamine was flowed twice over the activated CM5 sensor surface for 7 min, followed by injection of 400 μg/ml SPDP–collagen IV in a 10-mM sodium acetate buffer solution (pH 3.0) until the SPR response reached approximately 2000 response units (RU). When the collagen IV-immobilized sensor chip (collagen IV chip) needed to be regenerated, a 0.1-M borate buffer solution (pH 8.5) containing 0.10 M TCEP was injected onto the sensor chip at a flow rate of 5 μl/min for 15 min to cleave a disulfide bond by reduction.

The amount of immobilized collagen IV was changed by running a collagen IV solution for a different period at a constant flow rate (5 μl/min). The amount of immobilized collagen IV increased with the injection time (see Fig. S1 in supplementary material). This indicates that cysteamine sites on the sensor chip are not fully occupied by collagen IV given that the response is less than 2600 RU, and free cysteamine sites remain on the sensor chip. Considering the molecular size of collagen IV, the amount of collagen IV corresponding to 2000 RU was less than the amount required for the monolayer coverage (see supplementary material).

Monitoring of MMP-9 activity

First, a 1-μl portion of a full-length MMP-9 solution was diluted with 99 μl of a 50-mM Tris–HCl buffer solution (pH 7.4, abbreviated as a Tris solution) to give a 20-ng/ml solution. In addition, 100 ng/ml MMP-9 in a 50-mM Tris buffer (pH 7.4) solution containing 0.15 M NaCl and 0.005% Brij-35 (abbreviated as a Tris–NaCl–Brij solution) was also prepared by diluting 10 μl of a full-length MMP-9 solution with 190 μl of a Tris–NaCl–Brij solution. A catalytic domain solution of MMP-9 was prepared by diluting 4 μl of a catalytic domain solution with 196 μl of a Tris solution. These solutions were prepared immediately before their uses and diluted further if necessary.

After the surface of a collagen IV chip was equilibrated with a Tris solution or a Tris–NaCl–Brij solution at a flow rate of 10 μl/min, a diluted MMP-9 solution (200-μl portion) was loaded into an autosampler and its 150-μl portion was injected automatically into a flow cell for 15 min. A change in SPR signals was monitored continuously, reflecting the cleavage of triple helical collagen IV by MMP-9 (Fig. 1). A decrease in the SPR signal at time t after the injection of an MMP-9 solution was defined as $\Delta RU_{MMP}(t)$. The maximum decrease in the SPR signal (ΔRU_{max}) corresponds to complete digestion of surface collagen IV. The ΔRU_{max} values were determined to be 650 RU for MMP-9 in a Tris solution and also in a Tris–NaCl–Brij solution, and the value for MMP-9 CAT in a Tris solution was 800 RU by injecting 5 ng/ml MMP-9 and 400 ng/ml MMP-9 CAT in a Tris solution on a collagen IV chip, respectively. The SPR signal change was regarded as a plateau after 30 min. The response at 15 min after injection of MMP-9 [i.e., ΔRU_{MMP}(15 -min)] for MMP-9 (100 ng/ml) in a Tris–NaCl–Brij solution was almost constant for flow rates ranging from 2 to 20 μl/min (see Fig. S2 in supplementary material). This indicates that mass transport has a negligible role in determining the magnitude of ΔRU_{MMP}(15 min).

Kinetic parameter analysis

Kinetic parameters of MMP-9 activity were analyzed according to the method reported for oligonucleotides/RNase by Corn and coworkers [41–43]. If the fractional surface overages for surface species—a substrate (S), a surface enzyme–substrate complex (ES), and a surface product (S*)—are denoted as θ_S, θ_{ES}, and θ_{S*}, respectively, the kinetics of the enzymatic reaction are governed by the following equations:

$$\theta_S + \theta_{ES} + \theta_{S*} = 1 \tag{1}$$

$$\frac{d\theta_{ES}}{dt} = \frac{k_a[E](1 - \theta_{ES} - \theta_S*) - (k_d + k_{cat})\theta_{ES}}{1 + \beta(1 - \theta_{ES} - \theta_{S*})} \tag{2}$$

$$\frac{d\theta_{S*}}{dt} = k_{cat}\theta_{ES} \tag{3}$$

where $[E]$ is the bulk enzyme concentration, k_a and k_d are the Langmuir adsorption and desorption rate constants, respectively, k_{cat} is the surface reaction rate for the enzyme complex, and β is a dimensionless diffusion parameter. The fractional surface coverage (θ_{S*}) of the product at time t was calculated from the ratio of $\Delta RU_{MMP}(t)$ to ΔRU_{max}. Based on Eq. 3, a θ_{S*} versus t plot was constructed and its slope was obtained by finite difference analysis in the time range from $(t - \Delta 5s)$ to $(t + \Delta 5s)$, yielding a plot of $k_{cat}\theta_{ES}$ versus t. According to Corn and coworkers, the fraction λ_{ES} of unreacted surface sites that are occupied by the enzyme is given by

$$\lambda_{ES} = \frac{\theta_{ES}}{\theta_{ES} + \theta_S} = \frac{\theta_{ES}}{1 - \theta_{S*}} \tag{4}$$

A plot of $k_{cat}\lambda_{ES}$ versus t was constructed from λ_{ES} calculated based on Eq. 4 and θ_{S*} and $k_{cat}\theta_{ES}$ at time t. The value of λ_{ES} rises and reaches a steady-state one, as can be expressed by the following quadratic equation [41–43]:

$$\lambda_{ES} = \frac{-k_a[E]}{k_{cat}\lambda_{ES}} + \frac{(k_a[E] + k_d + k_{cat})}{k_{cat}} \tag{5}$$

The variation of λ_{ES} at a steady state depends on the bulk enzyme concentration $[E]$ because k_a, k_d, and k_{cat} are physical constants. Therefore, we rewrite this equation as follows:

$$[E] = \frac{k_{cat}\lambda_{ES}(k_{cat}\lambda_{ES} - k_d - k_{cat})}{k_a(k_{cat}\lambda_{ES} - k_{cat})} \tag{6}$$

Based on Eq. 6, the kinetic parameters k_a, k_d, and k_{cat} of MMP-9 can be obtained from the theoretical fits of an $[E]$ versus $k_{cat}\lambda_{ES}$ plot. The obtained SPR signal data were processed by Microsoft Excel software, and kinetic model fitting was performed using Wolfram Mathematica 7 software.

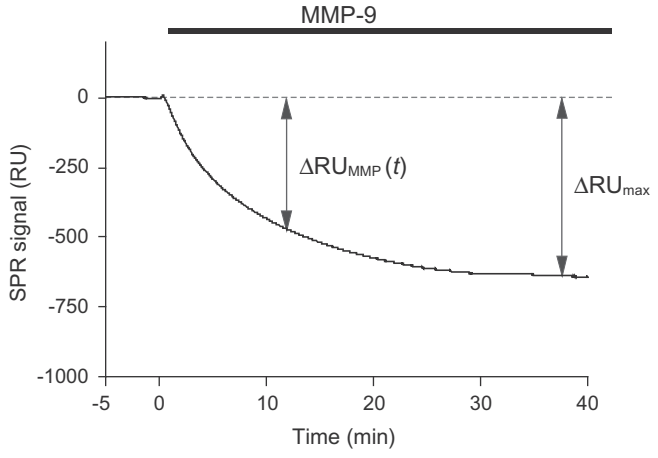

Fig.1. Time profile of SPR signal resulting from collagenolysis by MMP-9. The surface of a collagen IV-immobilized sensor chip (2000 RU) was equilibrated with a 50-mM Tris buffer solution (pH 7.4) at a flow rate of 10 μl/min, and then 5 ng/ml MMP-9 in the same buffer was injected onto a collagen IV chip. The closed bar indicates the period at which an MMP-9 solution was injected. The decrease in SPR signal is defined as $\Delta RU_{MMP}(t)$. ΔRU_{max} is the maximum decrease in the SPR signal that corresponds to complete digestion of surface collagen IV.

Results and discussion

Triple helical conformation of SPDP–collagen IV

Because collagen IV was necessary to be activated for the purpose of its immobilization on a cysteamine-modified sensor chip (cysteamine chip), whether or not the activated collagen IV maintains its triple helical structure is important for the measurement of MMP-9 collagenolytic activity. CD spectroscopy was used for characterizing the structure of collagen IV with or without SPDP modification (Fig. 2). A maximum molar ellipticity (θ) of native collagen IV and SPDP–collagen IV at room temperature was observed at 221 nm (inset in Fig. 2), indicating that the both collagen IV species are in triple helical conformation [1,2]. The thermal stability of collagen IV was monitored using a CD thermal denaturation experiment. Attenuation of the 221-nm spectral feature is known to represent a loss of the secondary structure content of the triple helical collagen structure. The thermal stability of triple helical conformation of collagen IV was unaffected by SPDP modification as judged from the thermal transition curves that overlapped each other for both collagens. In addition, it was confirmed that SPDP–collagen IV

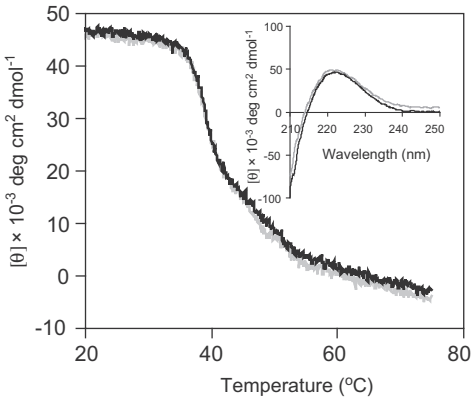

Fig.2. Thermal transition curves for native collagen IV (black line) and SPDP–collagen IV (gray line) in a 50-mM Tris buffer solution. Molar ellipticities ([θ]) were recorded at λ = 221 nm, whereas the temperature was increased from 20 to 75 °C at a rate of 0.2 °C/min. The inset shows CD spectra of native collagen IV (black line) and SPDP–collagen IV (gray line) at room temperature.

in a Tris solution (pH 7.4) at 37 °C maintained collagen-specific triple helical conformation.

Reusable sensor chip

To allow the reuse of a collagen IV chip, cleaving a disulfide bond that links SPDP–collagen IV to the surface of a cysteamine chip was investigated. The changes in the SPR signals for treatment with the reducing agent TCEP and reimmobilization of SPDP–collagen IV are shown in Fig. 3 At the first run, a 10-mM sodium acetate buffer solution (pH 3.0) containing 0.4 mg/ml SPDP–collagen IV was injected. The SPR signal exhibited a rapid rise, reaching a steady value of approximately 1050 RU at 1 min after the end of injection. Then 0.10 M TCEP in 0.1 M borate buffer solution (pH 8.5) was run for 15 min, followed by the injection of a borate buffer solution for 5 min. After the end of the injection, the SPR signal returned to the initial level before running collagen IV. This indicates that SPDP–collagen IV was stripped off from the surface of the sensor chip owing to cleavage of disulfide bonds that link collagen IV to the sensor surface. The successive immobilization of SPDP–collagen IV at the second and third runs gave a similar magnitude of the SPR signal, suggesting that the collagen IV chip can be reused after treating with TCEP.

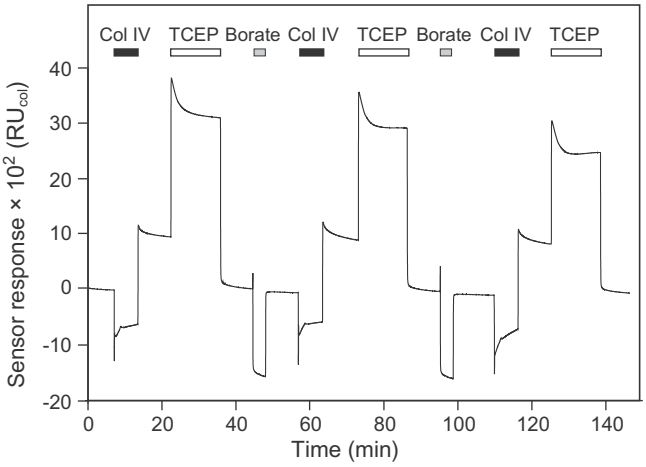

Fig.3. Time profiles of the SPR signal for immobilization of SPDP–collagen IV and treatment with the reducing agent TCEP. A running buffer was an HBS–EP solution at a flow rate of 10 μl/min. Closed bars indicate the periods at which 0.40 mg/ml SPDP–collagen IV in a 10-mM sodium acetate buffer solution (pH 3.0) was injected. Open bars indicate the injection of 0.1 M TCEP in a 0.1-M borate buffer solution (pH 8.5) for 15 min. Col IV, collagen IV. Gray bars indicate the injection of a 0.1-M borate buffer solution (pH 8.5) for 5 min.

Nonspecific interaction between MMP-9 and a cysteamine chip

In the current method, evaluating collagenolytic activity of MMP-9 relies on the specific interaction between MMP-9 in a solution and collagen IV immobilized on a cysteamine chip. Even though collagen IV was immobilized, some fraction of cysteamine sites will remain free on the sensor chip (see above). Such adsorption on a cysteamine chip can be detected as an increase in the SPR signal. The effect of buffer components on the adsorption of MMP-9 was investigated by injecting MMP-9 in a Tris solution with or without NaCl and Brij-35. A Tris solution with NaCl and Brij-35 has been used for minimizing a nonspecific interaction in MMP assay using synthetic triple helical peptides (THPs) [27–33].

Change (an increase) in the SPR signal (defined as ΔRU_{NS}) measured at 1 min after the end of MMP-9 injection on a cysteamine chip is given Table 1. In the case of a Tris solution, the injection of MMP-9 (100 ng/ml) caused an increase in ΔRU_{NS}, showing that the adsorption of MMP-9 on the sensor surface occurred. However, with a Tris solution containing both NaCl and Brij-35, ΔRU_{NS} was very small even for MMP-9 at high concentration, indicating that the nonspecific adsorption of MMP-9 is negligible in this medium. In the absence of NaCl and Brij-35, the nonspecific adsorption was suppressed by using a small concentration (5 ng/ml) of MMP-9. Consequently, the nonspecific adsorption of MMP-9 on a cysteamine chip is negligible if a Tris solution containing both NaCl and Brij-35 or a low concentration of MMP-9 is used.

Real-time measurement for MMP-9 collagenolytic activity

The real-time measurement of collagenolytic activity of MMP-9 that degrades triple helical collagen IV was performed with a collagen IV chip. After collagen IV was immobilized (2000 RU), MMP-9 in a Tris–NaCl–Brij solution with or without EDTA was injected. The time profiles of the SPR signal are shown in Fig. 4A. When 100 ng/ml MMP-9 in a Tris–NaCl–Brij solution was injected, the SPR signal decreased gradually with time up to 15 min (trace 1 in Fig. 4A). The ΔRU_{MMP}(15 min) was approximately 130 RU, corresponding to 20% of complete digestion. Such a decrease in the SPR signal was not observed when EDTA, an inhibitor for MMP-9, was present in a Tris–NaCl–Brij solution (trace 2). These results indicate that the time-dependent decrease in the SPR signal by injection of MMP-9 was due to its collagenolytic activity that degrades collagen IV immobilized on the sensor chip. The response 15 min after MMP-9 injection became larger with an increase in MMP-9 concentration ranging from 25 to 100 ng/ml, as shown in Fig. 4B. The lower detection limit of the collagenolytic activity measurement was 4.9 ng/ml, as calculated from ΔRU_{MMP}(15 min) at three times the standard deviation of the SPR signals in the absence of MMP-9.

Compared with the case of a Tris–NaCl–Brij solution, the SPR signal obtained by injecting MMP-9 at low concentration (10 ng/

Table 1
Nonspecific adsorption of MMP-9 on a cysteamine-modified sensor chip.

	Tris		Tris–NaCl	Tris–Brij	Tris–NaCl–Brij
	100 ng/ml	5 ng/ml			
ΔRU_{NS} (RU)	660 ± 120	4 ± 3	180 ± 70	220 ± 40	8 ± 4

Note: ΔRU_{NS} indicates an increase in SPR signal at 1 min after the end of MMP-9 injection. ΔRU_{NS} for Tris–NaCl, Tris–Brij, and Tris–NaCl–Brij were measured at an MMP-9 concentration of 100 ng/ml.

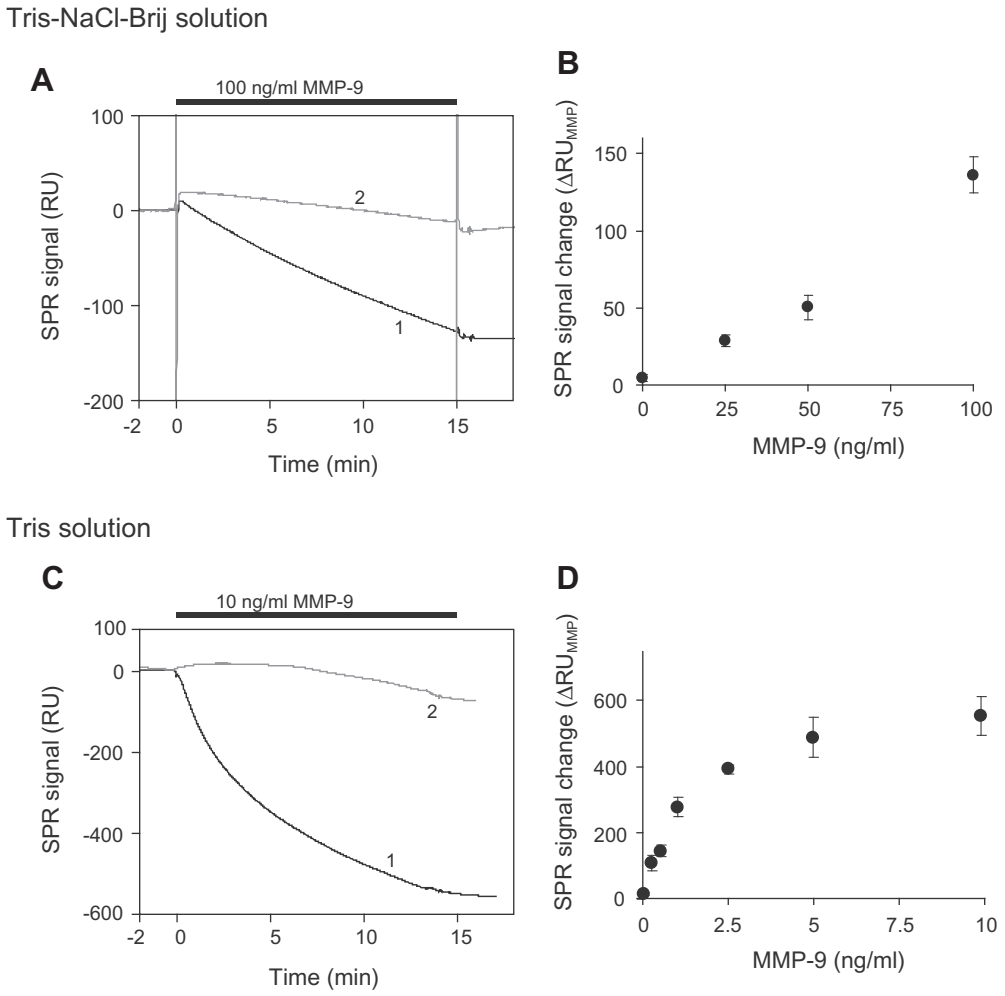

Fig.4. (A,C) Time profiles of the SPR signal caused by injection of MMP-9 in a Tris–NaCl–Brij solution (A) and in a Tris solution (C) with or without EDTA onto a collagen IV chip at a flow rate of 10 μl/min. The closed bar in each panel indicates the period at which an MMP-9 solution was injected. (B,D) Concentration dependencies for ΔRU_{MMP} at 1 min after injection of MMP-9 in a Tris–NaCl–Brij solution (B) and in a Tris solution (D). Averages of three measurements are plotted. Error bars indicate means ± standard deviations ($n = 3$).

ml) in a Tris solution decreased rapidly, and then the change in the SPR signal decreased gradually (trace 1 in Fig. 4C), suggesting that collagenolysis of MMP-9 in a Tris solution progressed faster than that in a Tris–NaCl–Brij solution. The ΔRU_{MMP}(15 min) corresponded to 83% of complete digestion, whereas it was suppressed when EDTA was present (trace 2 in Fig. 4C). The ΔRU_{MMP}(15 min) value increased with an increase in MMP-9 concentration ranging from 0.25 to 5 ng/ml (Fig. 4D). The detection limit (signal/noise [S/N] = 3) of the collagenolytic activity was 7×10^{-2} ng/ml, which is superior by two orders of magnitude to that in a Tris–NaCl–Brij solution. This suggests that the collagenolytic activity of MMP-9 in a Tris solution is higher than that in a Tris–NaCl–Brij solution.

For both cases, the ΔRU_{max} values did not indicate the amount of the collagen IV on the sensor surface (2000 RU) because residual collagen IV on a sensor chip after the MMP-9 reaction cannot be removed owing to formation of a disulfide crosslink. Wangkam and coworkers [36] reported that the physical adsorption of protein substrate on sensor surface is more suitable for the measurements of proteolytic activities than the covalent binding. However, in the current case, a covalent crosslink appeared to be essential for the stability of baseline before MMP-9 injection, leading to the reliable measurements of MMP-9 kinetic parameters.

MMP-9 is able to bind to collagen IV through fibronectin type II repeats motif (collagen binding domain) and C-terminal hemopexin-like domain [9–11,44], whereas EDTA inhibits Zn(II) sites existing within the catalytic domain. A complex between the EDTA-inhibited MMP-9 and collagen IV may be formed on the sensor surface, which may cause an increase in the SPR signal. However, this possibility was excluded because the injection of MMP-9 with EDTA showed no noticeable increases in the SPR signal. We speculate that the concentration of the complex on the surface of the sensor chip was very small. Consequently, the decrease in the SPR signal observed above by injection of MMP-9 in a Tris–NaCl–Brij solution or MMP-9 at low concentration in a Tris solution solely reflects the fractional surface coverage of the MMP-9 collagenolysis product.

Kinetic analysis for MMP-9 activity

There are few studies on estimation of kinetic parameters for MMP-9 [29,32,44]. Gioia and coworkers reported the k_{cat} and K_m of the enzymatic digestion of α2 chain within collagen IV using SDS–PAGE separation of collagen IV processed by MMP-9 under reducing conditions [44]. MMP-9 kinetic parameters have also been obtained using THPs as a collagen-like synthetic peptide [29,32]. However, kinetic parameters of MMP-9 for digestion of triple helical collagen IV have not been reported.

The kinetic parameters of MMP-9 for collagenolytic activity in a Tris solution and a Tris–NaCl–Brij solution were evaluated. Because nonspecific adsorption was negligible at low concentration of MMP-9 (see above), the measurements were carried out with MMP-9 in the concentration range from 0 to 100 ng/ml in a Tris–NaCl–Brij solution and from 0 to 5 ng/ml in a Tris solution. To obtain kinetic parameters, the fractional surface coverage $\theta_{S*}(t)$ of the product was calculated from the experimental time profiles of the SPR signal (see Fig. S3 in supplementary material). Then dependence of $k_{cat}\lambda_{ES}$ on t was obtained from the slope of the $\theta_{S*}(t)$ versus t plot, according to Eq. 3. The $k_{cat}\lambda_{ES}$ values at the equilibrium were plotted against the MMP-9 concentration and fitted to Eq. 6 (Fig. 5), yielding kinetic parameters of MMP-9 collagenolytic activity.

The kinetic parameters obtained are given in Table 2. The catalytic constants (k_{cat}) in Tris and Tris–NaCl–Brij solutions gave almost the same value, indicating that the presence of NaCl and Brij-35 does not affect the turnover of MMP-9. On the other hand, the association rate constant (k_a) of MMP-9 in a Tris–NaCl–Brij solution was significantly smaller than that in a Tris solution, indicating that the affinity of MMP-9 to collagen IV was decreased by the presence of NaCl and Brij-35. The isoelectric point (p*I*) of α-chain composing collagen IV, calculated using the algorithm from ExPASy's Compute pI/Mw program, was in the range from 8.5 to 9.2, whereas that of MMP-9 was p*I* = 5.5 (calculated). Hence, the presence of NaCl at high concentration is likely to suppress the electrostatic interaction between positively charged MMP-9 and negatively charged collagen IV. In addition, the concentration (0.05%) of Brij-35 in aqueous solution was beyond its critical micelle concentration (CMC = 90 μM) [34]. It has been reported that Brij-35 inhibits the activity of MMP-9 when its concentration exceeds CMC [16,34]. Taking these facts into consideration, we conclude that the high MMP-9 collagenolytic activity in a Tris solution is due to the higher affinity of MMP-9 to collagen IV.

In general, kinetic parameters obtained by heterogeneous enzymatic assays, where an enzyme in solution acts on an immobilized substrate, may differ from those observed in solution (homogeneous enzymatic assays) [42,45]. The kinetic parameters for MMP-9 determined by the current SPR method differ from those obtained by other homogeneous assay methods because substrate was different and collagen IV was on the sensor surface (Table 2).

Comparison of collagenolytic activity between full-length and catalytic domain of MMP-9

The collagenolytic activity of MMP-9 CAT in a Tris solution was compared with the activities of MMP-9. A ΔRU_{MMP}(15 min) versus concentration plot was linear for MMP-9 CAT in the range from 100 to 400 ng/ml with a lower detection limit (S/N = 3) of 6.0 ng/ml (see Fig. S4a in supplementary material). This indicates that MMP-9 CAT activity is significantly lower than that of MMP-9 (detection limit 7×10^{-2} ng/ml). The kinetic parameters of MMP-9 CAT were obtained in the same manner as for MMP-9 (Table 2). The results showed that k_a is significantly smaller as compared with that for MMP-9, whereas k_{cat} and k_d are the same. Thus, the removal of C-terminal hemopexin-like domain and the linker

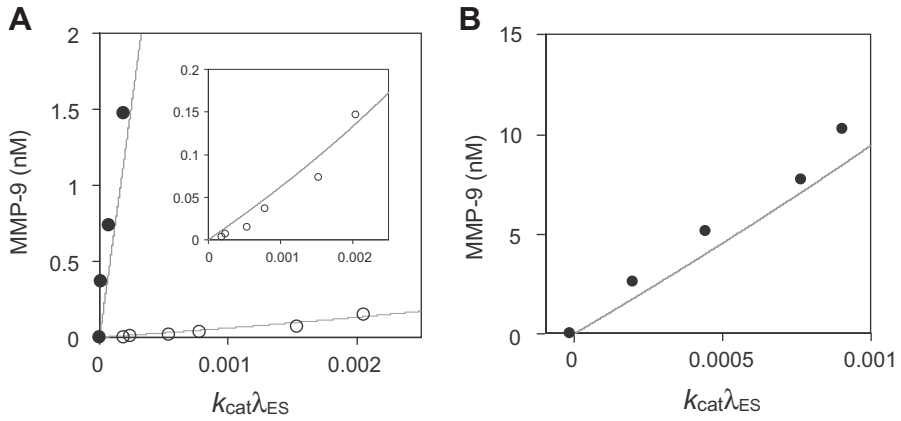

Fig.5. (A) Relationship between MMP-9 concentration and $k_{cat}\lambda_{ES}$ at the equilibrium in a Tris–NaCl–Brij solution (closed circles) and in a Tris solution (open circles). (B) Relationship between MMP-9 CAT concentration and $k_{cat}\lambda_{ES}$ at the equilibrium in a Tris solution. Averages of three measurements are plotted. The solid lines represent the theoretical fit of $k_{cat}\lambda_{ES}$ values to Eq. 6.

Table 2
Kinetic parameters for collagenolysis.

	Substrate	Buffer constituent	Kinetic parameters			
			k_a ($M^{-1}\,S^{-1}$)	k_d (S^{-1})	k_{cat} (S^{-1})	K_m (M)
SPR method (heterogeneous enzymatic assay)						
Full-length MMP-9	Collagen IV	Tris–NaCl–Brij	3.3×10^5	9.0×10^{-3}	9.0×10^{-3}	5.5×10^{-8}
		Tris	3.3×10^7	8.9×10^{-3}	9.3×10^{-3}	5.5×10^{-10}
MMP-9 CAT		Tris	2.7×10^5	0.8×10^{-2}	8.4×10^{-3}	7.5×10^{-8}
Electrophoresis (homogeneous enzymatic assay)						
MMP-9	α1 Chain [44]		ND	ND	1.2 ± 0.2	$1.0 \pm 0.1 \times 10^{-5}$
FRET-based assay (homogeneous enzymatic assay)						
MMP-9	Knight SSP [29]		ND	ND	6.22 ± 0.68	$2.77 \pm 0.6 \times 10^{-5}$
	fTHP-15 [32]		ND	ND	0.78 ± 0.13	$1.21 \pm 0.6 \times 10^{-5}$
	α1 (V) 436–447 fTHP [29]		ND	ND	0.0441	0.81×10^{-5}

Note: ND, no data; FRET, fluorescence resonance energy transfer; Knight SSP, short single-stranded synthetic substrate; fTHP-15, THP as substrate degraded by all collagenolytic MMPs; α1 (V) 436–447 fTHP, THP model of the MMP-9 cleavage sites in types V and XI collagen.

region (O-glycosylated domain) from MMP-9 leads to a decrease in affinity to collagen IV, whereas the turnover of MMP-9 is unaffected. It has been reported that the deletion of C-terminal hemopexin-like domain and the linker region from MMP-9 is less effective in decreasing affinity (K_m) to THPs [29]. A potential explanation for this difference is that there was a difference in amino acid sequence and length between the two substrates. The full-length collagen IV as a substrate has significantly larger molecular length (300 nm) than THPs. Overall and Butler reported that extension and retraction of flexible linker domain would allow the enzyme to inch along the collagen scanning for its cleavage recognition sequence [46,47]. Therefore, the processes for native collagen IV recognition by MMP-9 are likely to differ from those for THPs.

Conclusions

The current SPR biosensor is based on a decrease in the SPR signal resulting from the cleavage of full-length collagen IV as a substrate on the sensor surface. The SPR method allows us to evaluate enzymatic kinetic parameters of MMP-9 for full-length collagen IV. The kinetic parameters revealed that the higher collagenolytic activity of full-length MMP-9 as compared with that of its catalytic domain is ascribable to the high binding affinity of MMP-9 to collagen IV. This shows that the interplay among hemopexin-like domain, fibronectin type II repeats motif, and O-glycosylated domain increases the binding affinity of MMP-9 to collagen IV. The SPR method does not require denature and renature processes for MMP-9 and collagen IV; hence, the method is expected to provide reliable kinetic parameters of MMP-9 for collagenolysis. The current approach can be applied to the measurements of collagenolytic activity of other MMP family members.

Acknowledgments

We thank Yoichi Shibusawa and Akio Yanagida (Tokyo University of Pharmacy and Life Science) for the kind help of CD measurements. This work was financially supported by a Grant-in-Aid for Scientific and Research (B) (21350045) from the Ministry of Education, Culture, Sports, Science, and Technology of Japan.

Appendix A. Supplementary data

Supplementary data associated with this article can be found, in the online version, at doi:10.1016/j.ab.2011.07.031.

References

[1] G.N. Ramachandran, Molecular structure of collagen, Intl. Rev. Connect. Tissue Res. 1 (1963) 127–182.
[2] R.D.B. Fraser, T.P. Macray, E. Suzuki, Chain conformation in the collagen molecule, J. Mol. Biol. 129 (1979) 463–481.
[3] C. Busti, E. Falcinelli, S. Momi, P. Gresele, Matrix metalloproteinases and peripheral arterial disease, Intern. Emerg. Med. 5 (2010) 13–25.
[4] G. Murphy, H. Nagase, Progress in the matrix metalloproteinase research, Mol. Aspects Med. 29 (2008) 290–308.
[5] M. Egeblad, Z. Werb, New functions for the matrix metalloproteinases in cancer progression, Nat. Rev. Cancer 2 (2002) 161–174.
[6] M. Björklund, E. Koivunen, Gelatinase-mediated migration and invasion of cancer cells, Biochim. Biophys. Acta 1755 (2005) 37–69.
[7] C. Lopez-Otin, L.M. Matrisian, Emerging roles of proteases in tumor suppression, Nat. Rev. Cancer 7 (2007) 800–808.
[8] M. Ram, Y. Sherer, Y. Shoenfeld, Matrix metalloproteinase-9 and autoimmune diseases, J. Clin. Immunol. 26 (2006) 299–307.
[9] H. Nagase, J.F. Woessener, Matrix metalloproteinases, J. Biol. Chem. 274 (1999) 21491–21494.
[10] H. Birkedal-Hansen, W.G.I. Moore, M.K. Bodden, L.J. Windsor, B. Birkedal-Hansen, A. DeCarlo, J.A. Engler, Matrix metalloproteinases: A review, Crit. Rev. Oral Biol. Med. 4 (2010) 197–250.
[11] N. Sela-Passwell, G. Rosenblum, T. Shoham, I. Sagi, Structural and functional bases for allosteric control of MMP activities: Can it pave the path for selective inhibition? Biochim. Biophys. Acta 1803 (2010) 29-38
[12] C. Heussen, E.B. Dowdle, Electrophoretic analysis of plasminogen activators in polyacrylamide gels containing sodium dodecyl sulfate and copolymerized substrates, Anal. Biochem. 102 (1980) 196–202.
[13] P.A. Snoek-van Beurden, J.W. Von den Hoff, Zymographic techniques for the analysis of matrix metalloproteinases and their inhibitors, BioTechniques 38 (2005) 73–83.
[14] C. Lombard, J. Saulnier, J. Wallach, Assays of matrix metalloproteinases (MMPs) activities: A review, Biochimie 87 (2005) 265–272.
[15] J. Wilkesman, L. Kurz, Protease analysis by zymography: A review on techniques and patents, Recent Pat. Biotechnol. 3 (2009) 175–184.
[16] K. Kupai, G. Szucs, S. Cseh, I. Hajdu, C. Csonka, T. Csont, P. Ferdinandy, Matrix metalloproteinase activity assays: Importance of zymography, J. Pharmacol. Toxicol. Methods 61 (2010) 205–209.
[17] B. Gogly, N. Groult, W. Hornebeck, G. Godeau, B. Pellat, Collagen zymography as a sensitive and specific technique for the determination of subpicogram levels of interstitial collagenase, Anal. Biochem. 255 (1998) 211–216.
[18] D.E. Kleiner, W.G. Stetler-Stevenson, Quantitative zymography: Detection of picogram quantities of gelatinases, Anal. Biochem. 218 (1994) 325–329.
[19] G.W. Oliver, J.D. Leferson, W.G. Stetler-Stevenson, D.E. Kleiner, Quantitative reverse zymography: Analysis of picogram amounts of metalloproteinase inhibitors using gelatinase A and B reverse zymograms, Anal. Biochem. 244 (1997) 161–166.
[20] T.M. Leber, F.R. Balkwill, Zymography: A single-step staining method for quantitation of proteolytic activity on substrate gels, Anal. Biochem. 249 (1997) 24–28.
[21] S. Hattori, H. Fujisaki, T. Kiriyama, T. Yokoyama, S. Irie, Real-time zymography and reverse zymography: A method for detecting activities of matrix metalloproteinases and their inhibitors using FITC-labeled collagen and casein as substrates, Anal. Biochem. 301 (2002) 27–34.
[22] P. Fernández-Resa, E. Mira, A.R. Quesada, Enhanced detection of casein zymography of matrix metalloproteinases, Anal. Biochem. 224 (1995) 434–435.
[23] G.B. Fields, Using fluorogenic peptide substrates to assay matrix metalloproteinases, Methods Mol. Biol. 622 (2010) 393–433.
[24] C.G. Knight, F. Willenbrock, G. Murphy, A novel coumarin-labelled peptide for sensitive continuous assay of the matrix metalloproteinases, FEBS Lett. 296 (1992) 263–266.
[25] S.J. Kridel, E. Chen, L.P. Kotra, E.W. Howard, S. Mobashery, W. Smith, Substrate hydrolysis by matrix metalloproteinase-9, J. Biol. Chem. 276 (2001) 20572–20578.
[26] D.M. Bickett, M.D. Green, J. Berman, M. Dezube, A.S. Howe, P.J. Brown, J.T. Roth, G.M. McGeehan, A high throughput fluorogenic substrate for interstitial collagenase (MMP-1) and gelatinase (MMP-9), Anal. Biochem. 212 (1993) 58–64.
[27] L. Janelle, D.J. Lauer-Fields, G.B. Fields, Matrix metalloproteinases and collagen catabolism, Biopolymers 66 (2002) 19–32.
[28] D. Minond, J.L. Lauer-Fields, M. Cudic, C.M. Overall, D. Pei, K. Brew, R. Visse, H. Nagase, G.B. Fields, The roles of substrate thermal stability and P_2 and P_1 ' subsite identity on matrix metalloproteinase triple-helical peptidase activity and collagen specificity, J. Biol. Chem. 281 (2006) 38302–38313.
[29] J.L. Lauer-Fields, J.K. Whitehead, S. Li, R.P. Hammer, K. Brew, G.B. Fields, Selective modulation of matrix metalloproteinase-9 (MMP-9) functions via exosite inhibition, J. Biol. Chem. 283 (2008) 20087–20095.
[30] J.L. Lauer-Fields, T. Broder, T. Sritharan, L. Chung, H. Nagase, G.B. Fields, Kinetics analysis of matrix metalloproteinase activity using fluorogenic triple-helical substrates, Biochemistry 40 (2001) 5795–5803.
[31] J.L. Lauer-Fields, P. Kele, G. Sui, H. Nagase, R.M. Leblanc, G.B. Fields, Analysis of matrix metalloproteinase triple-helical peptidase activity with substrates incorporating fluorogenic L- or D-amino acids, Anal. Biochem. 321 (2003) 105–115.
[32] J.L. Lauer-Fields, T. Sritharan, M.S. Stack, H. Nagase, G.B. Fields, Selective hydrolysis of triple-helical substrates by matrix metalloproteinase-2 and -9, J. Biol. Chem. 278 (2003) 18140–18145.
[33] O. Gircz, J.L. Lauer, G.B. Fields, Comparison of metalloproteinase protein and activity profiling, Anal. Biochem. 409 (2010) 37–45.
[34] H.I. Park, S. Lee, A. Uliash, Q. Cao, Q-X.A. Sang, Effects of detergents on catalytic activity of human endometase/matrilysin 2, putative cancer biomarker, Anal. Biochem. 396 (2010) 262–268.
[35] U. Aldinger, P. Pfeifer, G. Schwotzer, P. Steinrücke, A comparative study of spectral and angle-dependent SPR devices in biological applications, Sens. Actuat. B 51 (1998) 298–304.
[36] T. Wangkam, T. Srikhirin, P. Wanachantararak, V. Baxi, B. Sutapun, R. Amarit, Investigation of enzyme reaction by surface plasmon resonance (SPR) technique, Sens. Actuat. B 139 (2009) 274–279.
[37] S.H. Jung, D.H. Kong, J.H. Park, S.T. Lee, J. Hyum, Y.M. Kim, K.S. Ha, Rapid analysis of matrix metalloproteinase-3 activity by gelatin arrays using a spectral surface plasmon resonance biosensor, Analyst 135 (2010) 1050–1057.
[38] K. Park, J. Ahn, S.Y. Yi, M. Kim, B.H. Chung, SPR imaging-based monitoring of caspase-3 activation, Biochem. Biophys. Res. Commun. 368 (2008) 684–689.
[39] Y. Inoue, T. Mori, G. Yamanoushi, X. Han, T. Sonoda, T. Niidome, Y. Katayama, Surface plasmon resonance imaging measurements of caspase reactions on peptide microarrays, Anal. Biochem. 375 (2008) 147–149.

[40] J.H. Kim, S. Roy, J.T. Kellis Jr., A.J. Poulse, A.P. Gast, C.R. Robertson, Protease adsorption and reaction on an immobilized substrate surface, Langmuir 18 (2002) 6312–6318.
[41] H.J. Lee, A.W. Wark, T.T. Goodrich, S. Fang, R.M. Corn, Surface enzyme kinetics for biopolymer microarrays: A combination of Langmuir and Michaelis–Menten concepts, Langmuir 21 (2005) 4050–4057.
[42] S. Fang, H.J. Lee, A.W. Wark, H.M. Kim, R.M. Corn, Determination of ribonuclease H surface enzyme kinetics by surface plasmon resonance imaging and surface plasmon fluorescence spectroscopy, Anal. Chem. 77 (2005) 6528–6534.
[43] H.J. Lee, A.W. Wark, H.M. Kim, R.M. Corn, Creating advanced multifunctional biosensors with surface enzymatic transformations, Langmuir 22 (2006) 5241–5250.
[44] M. Gioia, S. Monaco, P.E. Van Den Steen, D. Sbardella, G. Grasso, S. Marini, C.M. Overall, G. Opdenakker, M. Coletta, The collagen binding domain of gelatinase A modulates degradation of collagen IV by gelatinase B, J. Mol. Biol. 386 (2009) 419–434.
[45] O.A. Gutiérrez, M. Chavez, E. Lissi, A theoretical approach to some analytical properties of heterogeneous enzymatic assays, Anal. Chem. 76 (2004) 2664–2668.
[46] C.M. Overall, Molecular determinants of metalloproteinase substrate specificity: Matrix metalloproteinase substrate binding domains, modules, and exosites, Mol. Biotechnol. 22 (2002) 51–86.
[47] C.M. Overall, G.S. Butler, Protease yoga: Extreme flexibility of a matrix metalloproteinase, Structure 15 (2007) 1159–1161.